Available online at www.sciencedirect.com
ScienceDirect
International Journal of Heat and Mass Transfer 51 (2008) 517–525
International Journal of HEAT and MASS TRANSFER
www.elsevier.com/locate/ijhmt

Conjugate conduction-forced convection heat transfer analysis of a rectangular nuclear fuel element with non-uniform volumetric energy generation

M.K. Ramis, G. Jilani *, S. Jahangeer

Department of Mechanical Engineering, National Institute of Technology Calicut, Kerala 673 601, India

Received 1 December 2006; received in revised form 5 May 2007
Available online 31 July 2007

Abstract

The main objective of this paper is to present a comparative study of uniform and non-uniform volumetric energy generation in a rectangular nuclear fuel element washed by upward moving stream of liquid sodium. Employing finite difference schemes, the boundary layer equations governing the flow and thermal fields in the fluid domain are solved simultaneously with two-dimensional energy equation in the solid domain by satisfying the continuity of temperature and heat flux at the solid–fluid interface. Numerical results are presented for a wide range of aspect ratio, A_r, conduction–convection parameter, N_{cc}, total energy generation parameter, Q_t, and flow Reynolds number, Re_H. It is concluded that for the same total energy generation, a somewhat realistic non-uniform volumetric energy generation puts greater restriction on the thermal power generation as compared to the idealistic uniform volumetric energy generation. Further, it is found that despite the total energy generation being the same for two cases, the non-uniform volumetric energy generation within the fuel element results in considerably higher energy dissipation rate.

Keywords: Conjugate heat transfer; Nuclear fuel element; Finite difference schemes; Conduction–convection parameter; Total energy generation parameter

1. Introduction

The term 'conjugate heat transfer' refers to a heat transfer process involving an interaction of heat conduction within a solid body with either of the free, forced, and mixed convection from its surface to a fluid (or to its surface from a fluid) flowing past over it. Thus, a realistic analysis of conjugate heat transfer problems requires the coupling of the conduction problem in the solid with the convection problem in the fluid by satisfying the conditions of continuity in temperature and heat flux at the solid–fluid interface. There are many engineering applications wherein conjugate heat transfer analysis becomes essential. One of the most common examples is a heat exchanger in which the heat conduction in the tube wall is greatly influenced by the convection in the surrounding fluid. Another important example of conjugate heat transfer problem can be found in fins. The conduction within the fin and convection in the fluid surrounding it must be simultaneously analyzed to obtain vital design information. The conjugate heat transfer finds yet another very important application in the fuel element of a nuclear reactor. In order to maintain the maximum temperature within the fuel element below its allowable limit, the energy released due to fission in the fuel element is conducted to its lateral surface, which in turn is dissipated to the coolant flowing past over it by convection.

Owing to its important engineering applications as mentioned above, conjugate heat transfer analysis of heat dissipating cylindrical as well as rectangular elements with volumetric energy generation has been the subject of many

* Corresponding author. Tel.: +91 495 2286402; fax: +91 495 2287250.
E-mail address: jilani@nitc.ac.in (G. Jilani).

0017-9310/$ - see front matter © 2007 Elsevier Ltd. All rights reserved.
doi:10.1016/j.ijheatmasstransfer.2007.05.019

Nomenclature

A_r	aspect ratio of the fuel element, $\frac{H}{2W}$
C	geometric parameter, $4A_r^2$
C_p	specific heat of the coolant
C_r	ratio of thermal conductivity of fuel element to that of coolant, $\frac{k_s}{k_f}$
h_{avg}	average heat transfer coefficient
H	height of the fuel element
k_f	thermal conductivity of the coolant
k_s	thermal conductivity of fuel element material
N_{cc}	conduction–convection parameter, $\frac{k_f}{k_s}\left[\frac{W}{H}\right]$
Nu_H	average Nusselt number, $\frac{h_{avg}H}{k_f}$
Pr	Prandtl number, $\frac{\nu}{\alpha}$
$q'''(x)$	volumetric energy generation function
q'''_{max}	maximum volumetric energy generation
$Q(X)$	dimensionless volumetric energy generation function, $\frac{q'''(x)W^2}{k_s(T_0-T_\infty)}$
Q_{max}	maximum volumetric energy generation parameter, $\frac{q'''_{max}W^2}{k_s(T_0-T_\infty)}$
Q_t	total energy generation parameter
Re_H	flow Reynolds number, $\frac{U_\infty H}{\nu}$
T	temperature
T_0	maximum allowable temperature in the fuel element
u	velocity component in the axial direction
U	dimensionless velocity component in the axial direction, $\frac{u}{U_\infty}$
U_∞	free stream velocity
v	velocity component in the transverse direction
V	dimensionless velocity component in the transverse direction, $\frac{v}{U_\infty}$
x	axial co-ordinate
X	dimensionless axial co-ordinate, $\frac{x}{H}$
y	transverse co-ordinate
Y_f	dimensionless transverse co-ordinate with respect to fluid domain, $\frac{y}{H}$
Y_s	dimensionless transverse co-ordinate with respect to solid domain, $\frac{y}{W}$
W	half of the thickness of the fuel element
ΔY_f	grid size in transverse direction of the fluid domain

Greek symbols

θ	dimensionless temperature, $\frac{(T-T_\infty)}{(T_0-T_\infty)}$
α	thermal diffusivity of the coolant
ρ	density of the coolant
μ	dynamic viscosity of the coolant
ν	kinematic viscosity of the coolant

Subscripts

f	fluid domain
s	solid domain
sf	solid–fluid interface
∞	free stream

investigations until recent past. Perelman [1] was probably the first to study analytically the conjugate heat transfer problem associated with the forced convection flow over a thin plate with volumetric heat source. Karvinen [2] presented an approximate method for solving the conjugate heat transfer problem associated with a heat generating plate washed by forced convection flow. Velusamy and Garg [3] numerically studied the transient natural convection over heat generating vertical cylinder by neglecting axial conduction in the cylinder and lumping the temperature of the cylinder in the radial direction. Wang and Georgiadis [4] numerically simulated the problem of conjugate forced convection in cross flow over an array of cylinders with uniform volumetric heat generation. Recently, Jilani et al. [5] numerically studied the conjugate heat transfer problem associated with a heat generating vertical cylinder washed by upward forced flow of low Prandtl number fluid. Most recently, Jahangeer et al. [6] carried out a numerical study on the conjugate heat transfer problem pertinent to laminar forced convection flow over a vertical plate having uniform volumetric energy generation.

An up-to-date review of the literature presented above reveals that with the exception of Perelman [1], Karvinen [2], and Jahangeer et al. [6], none of the investigators paid their attention to the conjugate heat transfer analysis of heat generating plate. While the analytical treatment of Perelman [1] is limited to specific cases without any parametric study, the analytical study presented by Karvinen [2] is based on one-dimensional heat conduction in the heat generating plate. On the other hand, the parametric study reported by Jahangeer et al. [6] is limited to a uniform volumetric heat generation in the vertical plate, which is somewhat idealistic. Some of these inadequacies of the previous investigations are the main source of motivation of the present work, which mainly presents a comparative study of the heat transfer characteristics of a rectangular nuclear fuel element having realistic non-uniform volumetric energy generation with those of idealistic ones.

2. Mathematical formulation

Fig. 1 shows a rectangular nuclear fuel element of height H, thickness $2W$ and thermal conductivity k_s washed by upward flowing liquid sodium as coolant having densityρ, dynamic viscosity μ, specific heat C_p, and thermal conductivity k_f. The upstream conditions of the coolant are maintained at uniform temperature T_∞ and uniform velocity U_∞. A Cartesian coordinate system is superimposed on

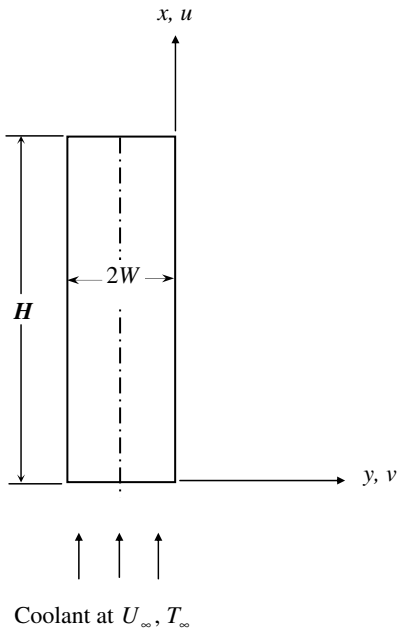

Fig. 1. Physical model.

the fuel element in such a manner that its origin coincides with the bottom-right corner of the fuel element and its x-coordinate is marked upward along the solid–fluid interface while its y-coordinate is directed towards right direction as shown in the figure. Under steady state operating conditions of the nuclear reactor, while the leading edge of the fuel element is assumed to be in perfect thermal contact with the oncoming stream of coolant, thereby, maintained at temperature T_∞, the heat dissipation from its trailing edge is considered negligibly small. The volumetric energy generation q''' due to fission in the fuel element is considered to be non-uniform along its axial direction. The energy generated in the fuel element is first conducted within it and finally dissipated from its lateral surface by forced convection to the upward moving streams of coolant so as to keep the maximum temperature T_0 in the fuel element well within certain permissible limit. For the mathematical formulation of the physical problem stated above, the following additional approximations and assumptions are introduced:

(i) The material of the fuel element is homogeneous and isotropic.
(ii) The thermal conductivity of the fuel element is independent of temperature.
(iii) The temperature gradient normal to the x–y plane is negligibly small.
(iv) The flow is steady, laminar, incompressible and two-dimensional.
(v) The coolant is Newtonian and viscous.
(vi) The thermo-physical properties of the coolant are constant.
(vii) The boundary layer approximations are valid.

From the physical model described above, it is abundantly clear that the temperature profile in the fuel element as well as temperature and velocity profiles in the coolant flowing over it are symmetric about the vertical axis of the fuel element due to geometric, thermal and fluid flow symmetry. Therefore, only half of the solution domain needs to be taken as the computational domain. The differential equation and the boundary conditions governing the steady, two-dimensional temperature distribution in the fuel element can be obtained in dimensionless form as:

$$\frac{\partial^2\theta_s}{\partial X^2}+C\frac{\partial^2\theta_s}{\partial Y_s^2}+CQ(X)=0 \tag{1}$$

$$\frac{\partial\theta_s(-1,X)}{\partial Y_s}=0;\quad \frac{\partial\theta_s(0,X)}{\partial Y_s}=N_{cc}\frac{\partial\theta_f(0,X)}{\partial Y_f}$$

$$\theta_s(0,X)=\theta_f(0,X)$$

$$\theta_s(Y_s,0)=0;\quad \frac{\partial\theta_s(Y_s,1)}{\partial X}=0 \tag{2}$$

The dimensionless volumetric energy generation function $Q(X)$ appearing in Eq. (1) is a cosine function of the axial coordinate X and can be expressed in dimensionless form as [7]

$$Q(X)=Q_{max}\cos\pi\left(\frac{1}{2}-X\right) \tag{3}$$

Introducing Prandtl's boundary layer approximation, the dimensionless form of the equations governing the flow and thermal field in the fluid domain can be obtained as [6]

$$\text{Continuity:}\quad \frac{\partial U}{\partial X}+\frac{\partial V}{\partial Y_f}=0 \tag{4}$$

$$\text{X-momentum:}\quad U\frac{\partial U}{\partial X}+V\frac{\partial U}{\partial Y_f}=\frac{1}{Re_H}\frac{\partial^2 U}{\partial Y_f^2} \tag{5}$$

$$\text{Energy:}\quad U\frac{\partial\theta_f}{\partial X}+V\frac{\partial\theta_f}{\partial Y_f}=\frac{1}{Re_H Pr}\frac{\partial^2\theta_f}{\partial Y_f^2} \tag{6}$$

The most appropriate boundary conditions in their dimensionless form are

$$U(Y_f,0)=1,\quad V(Y_f,0)=0,\quad \theta_f(Y_f,0)=0,\quad U(0,X)=0,$$
$$V(0,X)=0,\quad U(\infty,X)=1,\quad \theta(\infty,X)=0 \tag{7}$$

It is important to emphasize here that the main objective of the present investigation is to carry out a comparative conjugate heat transfer study with respect to uniform and non-uniform volumetric energy generation in the fuel element of a typical nuclear reactor. Thus, in order to fulfill this objective on equitable terms, we have introduced a new parameter termed as 'total energy generation parameter' Q_t, which is obtained by integrating the volumetric energy generation function $Q(X)$ over the entire volume of the fuel element. Thus, total energy generation parameter Q_t is the natural choice to be taken as common input parameter for both uniform and non-uniform volumetric energy generation cases. However, in the non-uniform energy

generation case we need Q_{max} in Eq. (3), which can be expressed in terms of Q_t by the following relation:

$$Q_{max} = \frac{\pi}{2} Q_t \tag{8}$$

3. Numerical solution

Eqs. (4)–(6) for the fluid and Eq. (1) for the solid are coupled and, therefore, the solutions of these equations are obtained numerically by satisfying the conditions of continuity of temperature and heat flux at the solid–fluid interface. The boundary layer equations (Eqs. (4)–(6)) for the fluid being parabolic in nature, are solved using numerical marching technique solution procedure, while Line-by-Line Gauss–Seidel iterative method is employed for steady, two-dimensional heat conduction equation for the fuel element. Accordingly, while Eq. (4) is discretized so as to solve in an explicit stepwise manner, fully implicit finite difference scheme is used in the discretization of Eqs. (5) and (6). Following Hornbeck [8], Eqs. (5) and (6) are discretized using backward difference formulae for the X-derivatives and central difference formulae for Y_f-derivatives, whereas only backward difference formula for both X- and Y_f-derivatives is employed to obtain finite difference form of Eq. (4). It is worth emphasizing here that the finite difference forms of Eqs. (5) and (6) possess tridiagonal structure and, therefore, are solved efficiently using famous 'Thomas Algorithm'. The detailed numerical solution procedure adopted for the solution of the conjugate heat transfer problem pertinent to the present work is quite similar to the one described by Jilani et al. [5] and, therefore, is omitted here for the sake of brevity.

3.1. Validation of the computer code

The numerical results presented in this paper are computed using a computer code developed by the authors, which takes care of different kinds of boundary conditions at the solid boundaries and steady state heat conduction in the solid with and without volumetric energy generation. The validity of this code has been examined by comparing the temperature profiles at the solid–fluid interface obtained using the present code for a wide range of conductivity ratio C_r with those presented by Vynnycky et al. [9]. It is important to mention here that the numerical study presented by Vynnycky et al. [9] pertains to the conjugate heat transfer problem associated with steady, laminar forced convection flow of incompressible fluid over the upper surface of a conducting slab of both finite length and thickness with its leading and trailing edges assumed to be adiabatic and the lower surface maintained at an uniform temperature greater than that of oncoming free stream. It is also worth emphasizing here that their results are obtained from the solution of Full Navier–Stokes equations and energy equation. From the comparison depicted in Fig. 2, it can be easily noted that with the exception of

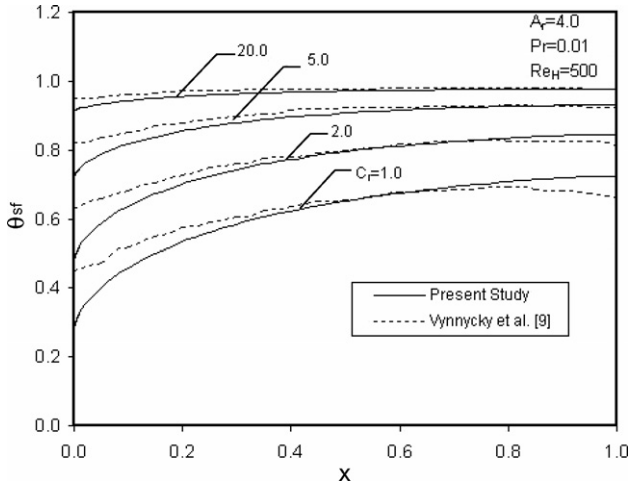

Fig. 2. Comparison of solid–fluid interface temperature profile with that of Vynnycky et al. [9] for different conductivity ratios.

temperature values near the leading edge, numerical results obtained using the present code is in good agreement with those reported by Vynnycky et al. [9]. Thus, the validity of the present code is established.

3.2. Grid independence test

The numerical results reported in this paper are obtained using optimum grid sizes, which are ascertained by numerical experimentation. As expected, it is observed that optimum grid sizes vary with flow Reynolds number, Re_H. Thus, different sets of numerical experimentation have been conducted for different value of Re_H. Figs. 3a and 3b illustrates one such grid independence test performed for $Re_H = 2500$ while $A_r = 10$, $N_{cc} = 0.35$, and $Q_t = 0.50$ are kept fixed. Fig. 3a shows the transverse temperature profiles at the axial location $X = 0.50$ in the fuel element for three different grid sizes, i.e., 21×358,

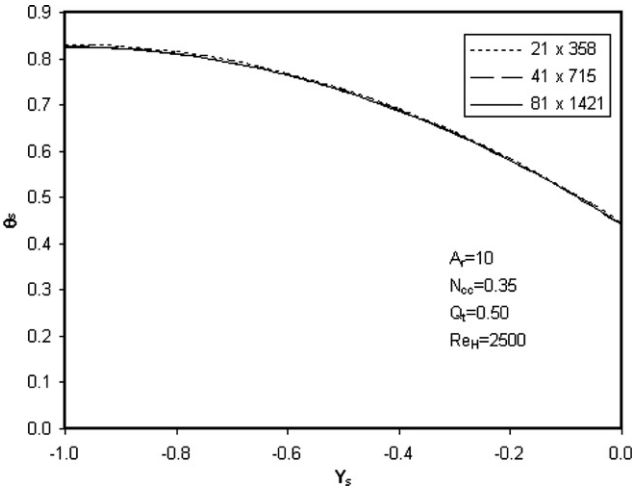

Fig. 3a. Transverse temperature profiles at $X = 0.5$ in the fuel element for three different grid sizes.

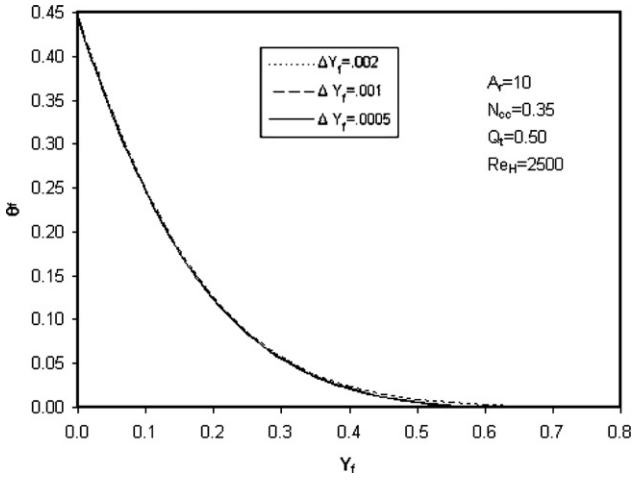

Fig. 3b. Transverse temperature profiles at $X = 0.5$ in the coolant for three different grid sizes.

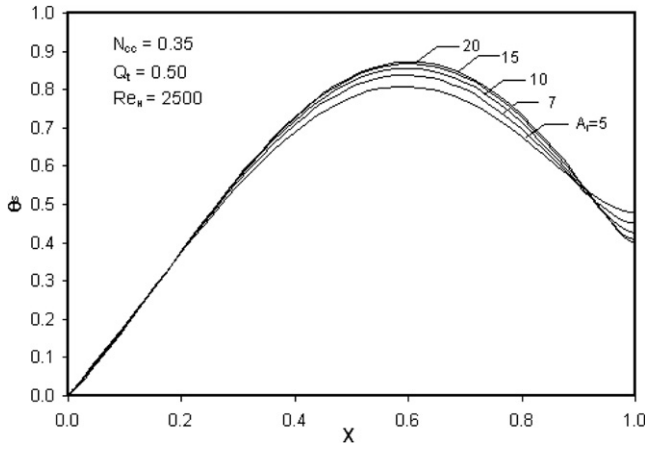

Fig. 4. The effect of A_r on axial temperature profiles along the vertical axis of the fuel element for fixed values of $N_{cc} = 0.35$, $Q_t = 0.50$, and $Re_H = 2500$.

41×715, and 81×1421. Similarly, Fig. 3b depicts the transverse temperature profiles at the same axial location $X = 0.50$ in the fluid domain for three different grid sizes taken very next to the solid–fluid interface along with variable grid pattern having successive grid sizes ratios same in all the three cases. It can be noticed from these figures that irrespective of the grid sizes used, all the three temperature profiles superimpose each other. However, taking into the consideration of better resolution of zero Neumann boundary conditions, a grid size of 41×715 in the solid domain and an initial value of $\Delta Y_f = 0.001$ in the fluid domain is chosen for $Re_H = 2500$.

4. Results and discussion

The objective of this paper is of twofold – the first to present a comparative study of uniform and non-uniform volumetric energy generation in a rectangular nuclear fuel element washed by upward moving liquid sodium and the second to ascertain the values of critical design parameters, which govern the optimum operating conditions of nuclear reactors with non-uniform volumetric energy generation. Accordingly, keeping the value of Prandtl number, Pr for liquid sodium to be constant at 0.005, at first, numerical results in the form of axial temperature profiles for non-uniform volumetric energy generation case alone are presented. Next, the comparative study of uniform and non-uniform volumetric energy generation in the fuel element in the form of variation of maximum temperature θ_{max} and average Nusselt number Nu_H for a wide range of aspect ratio A_r, total energy generation parameter Q_t, conduction–convection parameter N_{cc}, and Reynolds number Re_H are discussed in detail.

4.1. Axial temperature profiles

Fig. 4 illustrates the effect of A_r on axial temperature profile along the central line of the fuel element while $N_{cc} = 0.35$, $Q_t = 0.50$, and $Re_H = 2500$ are being kept fixed. It can be seen that the temperature in the fuel element first increases sharply along its axial direction, attains its maximum value very next to its midpoint, and there onwards decreases gradually up to the trailing edge. This is due to the fact that the volumetric energy generation in the fuel element varies along its axial direction with its maximum value at its middle. Further, it can be noticed that as A_r increases, the temperature in the region $0.25 \leqslant X \leqslant 0.85$ of the fuel element increases slightly with maximum increase occurring in the vicinity of its midpoint. In contrast to the preceding observation, it can be noticed that there exists a point near the trailing edge of the fuel element beyond which the temperature of the fuel element decreases with increase in A_r. Furthermore, it is important to note that for all values of $A_r \geqslant 15$, the effect of A_r on axial temperature profiles in the fuel element diminishes and as a result, all the profiles corresponding to $A_r \geqslant 15$ superimpose each other. The just preceding trend in the axial temperature profile due to increase in A_r, other parameters being kept fixed, may be attributed to the fact that for an increase in A_r beyond its certain value, the heat conduction in transverse direction predominates over that in axial direction and in effect, the heat transfer process in the fuel element becomes locally one-dimensional. Thus, it can be concluded that for a fixed set of parameters, there exists a maximum value of A_r beyond which the temperature of the fuel element becomes independent of A_r.

Fig. 5 shows the effect of N_{cc} on the axial temperature profile along the central line of the fuel element while keeping A_r, Q_t, and Re_H fixed at 10.0, 0.50, and 2500, respectively. It can be seen that unlike the effect of A_r on the axial temperature profile depicted in Fig. 4, the temperature everywhere in the fuel element along its axial direction decreases with increase in N_{cc}. Further, it must be noted that as N_{cc} decreases the maximum temperature in the fuel element increases monotonically and finally exceeds its allowable limit. This is due to the fact that for fixed value

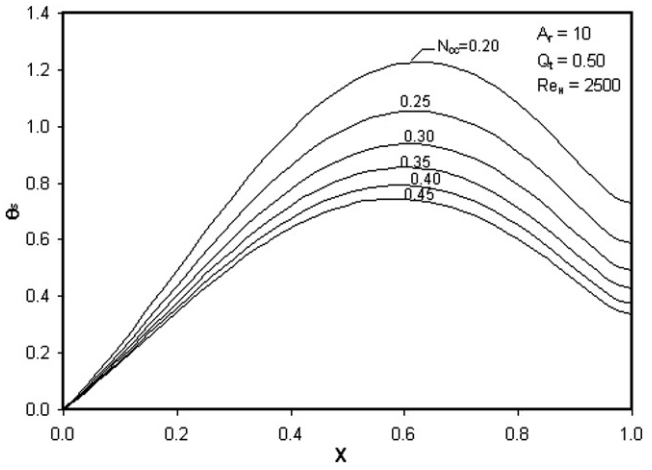

Fig. 5. The effect of N_{cc} on axial temperature profiles along the vertical axis of the fuel element for fixed values of $A_r = 10$, $Q_t = 0.50$, and $Re_H = 2500$.

of A_r and thermal conductivity of the fuel element, decrease in N_{cc} is essentially due to decrease in thermal conductivity of the coolant which lead to decrease in heat dissipation rate from the surface of the fuel element resulting in increase in fuel element temperature. In contrast to the above, it is evident from this figure that an increase in N_{cc} not only results in decrease in fuel element temperature, the rate of decrease in the fuel element temperature due to increase in N_{cc} also decreases sharply and ultimately becomes negligibly smaller and smaller. This too may be attributed to the fact that increase in N_{cc}, A_r and thermal conductivity of the fuel element being kept fixed, is due to increase thermal conductivity of the coolant which in turn facilitates higher heat dissipation rate resulting in decrease in fuel element temperature. However, thermal conductivity of the fuel element being kept fixed, there is a natural limit put on the heat dissipation rate from the surface of the fuel element beyond which it cannot be further increased. From the foregoing discussion, one can easily conclude that there exists a lower limiting value of N_{cc} below which temperature in the fuel element exceeds its allowable limit. Also, there exists an upper limiting value of N_{cc} beyond which its effect on the axial temperature profile becomes insignificant.

Fig. 6 depicts the effect of Q_t on the axial temperature profile along the central line of the fuel element while keeping A_r, N_{cc}, and Re_H fixed at 10.0, 0.35, and 2500, respectively. It can be seen that for all values of Q_t, the nature of the axial temperature profiles are quite similar to those demonstrated in Figs. 4 and 5. Further, it is quite important to note that for a set of fixed parameters; there exists an upper limiting value of Q_t beyond which the maximum temperature in the fuel element exceeds its allowable limit.

Fig. 7 illustrates the effect of Re_H on axial temperature profile along the central line of the fuel element while $A_r = 10.0$, N_{cc}= 0.35, and $Q_t = 0.50$ are being kept fixed. As expected, it is evident from this figure that an increase in Re_H results in a decrease in the maximum temperature in the fuel element. Further, it is interesting to note that there is an upper limiting value of Re_H beyond which an increase in Re_H results in insignificant decrease in fuel element temperature. Thus, it can be concluded that there is an upper limiting value of Re_H beyond which pumping power requirement of the coolant in the nuclear reactor increases unnecessarily. In contrast to the preceding observation, it is quite crucial to note from this figure that a small decrease in Re_H results in large increase in fuel element temperature. Since the fuel element temperature cannot be increased beyond its allowable limit, it puts a stringent restriction on further decrease in Re_H below its lower limiting value.

4.2. Maximum temperature profiles

Fig. 8 shows the variation of θ_{max} in the fuel element having non-uniform volumetric energy generation with A_r and

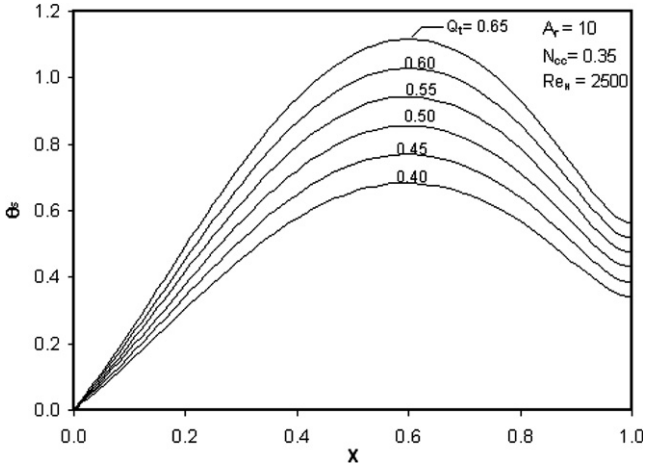

Fig. 6. The effect of Q_t on axial temperature profiles along the vertical axis of the fuel element for fixed values of $A_r = 10$, $N_{cc} = 0.35$, and $Re_H = 2500$.

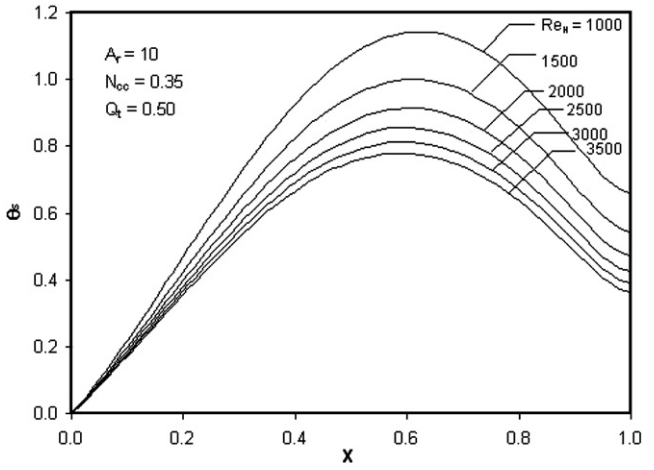

Fig. 7. The effect of Re_H on axial temperature profiles along the vertical axis of the fuel element for fixed values of $A_r = 10$, $N_{cc} = 0.35$, and $Q_t = 0.50$.

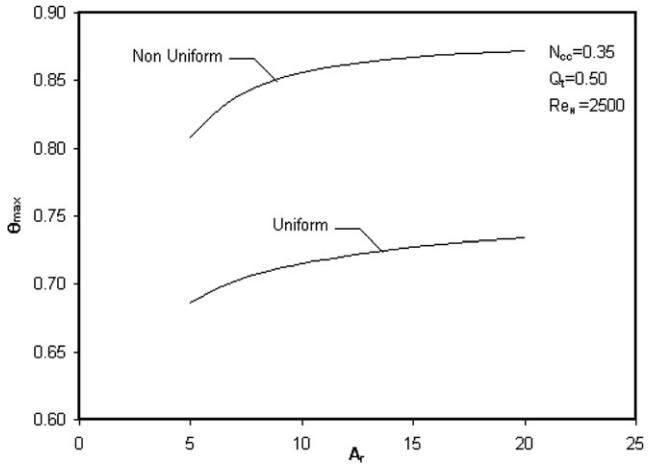

Fig. 8. Variation of the θ_{max} in the fuel element with A_r for both uniform and non-uniform heat generation cases, at fixed values of $N_{cc} = 0.35$, $Q_t = 0.50$, and $Re_H = 2500$.

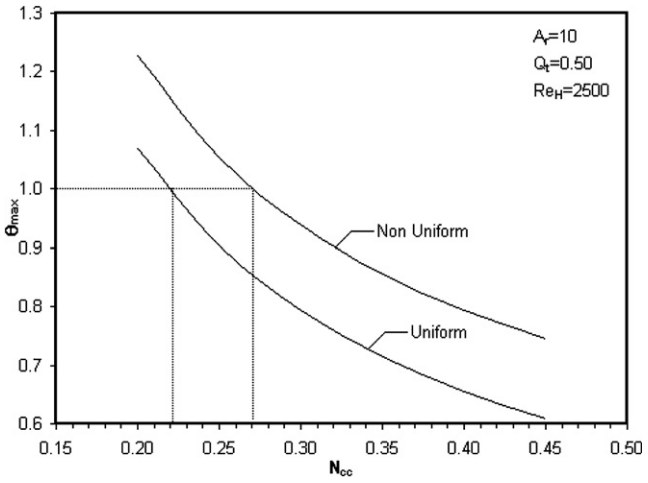

Fig. 9. Variation of the θ_{max} in the fuel element with N_{cc} for both uniform and non-uniform heat generation cases, at fixed values of $A_r = 10$, $Q_t = 0.50$, and $Re_H = 2500$.

its comparison with that of uniform volumetric energy generation case while the values of N_{cc}, Q_t, and Re_H are being kept fixed at 0.35, 0.50, and 2500, respectively. It is worth emphasizing here that Q_t represents the time rate of total energy generation due to fission in the fuel element, which is being kept at the same magnitude for both uniform and non-uniform energy generation cases. At first, it can be easily noticed from this figure that although, for both uniform as well as non-uniform energy generation in the fuel element, θ_{max} keeps on increasing with increase in A_r, increase in θ_{max} for initial lower values of A_r is somewhat significant as compared to those for its higher values. Next, it is important to note that irrespective of the values of A_r, θ_{max} values for non-uniform volumetric energy generation case, time rate of total energy generated being the same, is much higher than those for uniform volumetric energy generation case. Thus, it can be concluded that although the time rate of total energy generated within the fuel element due to fission is the same for both cases studied, a relatively more realistic non-uniform volumetric energy generation situation puts greater restriction on the power generation capacity of the nuclear reactor as compared to idealistic uniform volumetric energy generation case.

Fig. 9 depicts the variation of θ_{max} with N_{cc} for both uniform and non-uniform volumetric energy generation cases while $A_r = 10.0, Q_t = 0.50$, and $Re_H = 2500$ are being kept fixed. As expected, it can be noticed from this figure that for both uniform and non-uniform energy generation cases, θ_{max} decreases with increase in N_{cc}. Further, it is important to note that for a set of fixed parameters, θ_{max} corresponding to non-uniform volumetric energy generation is considerably higher than that of uniform energy generation case. Furthermore, it is worth noticing that the critical value of N_{cc} for non-uniform volumetric energy generation case is much higher than that of uniform volumetric energy generation case. Thus, one can easily conclude that although the non-uniform volumetric energy generation in the fuel element is somewhat realistic, it either puts certain restriction on the energy that would be generated in the fuel element of a nuclear reactor or demand higher rate of energy dissipation from the surface of the fuel element which, in turn, is related to pumping power requirement of the coolant.

Fig. 10 illustrates the variation of θ_{max} with Q_t for both uniform and non-uniform volumetric energy generation cases while $A_r = 10.0$, $N_{cc} = 0.35$, and $Re_H = 2500$ are being kept fixed. As expected, it is abundantly clear from this figure that θ_{max} increases monotonically with increase in volumetric energy generation. Quite similar to the observation made in the discussion of Figs. 8 and 9, it is to be noted from this figure as well that for any fixed value of Q_t, other parameters being kept fixed, θ_{max} with non-uniform volumetric energy generation is much higher than that of uniform volumetric energy generation case. Moreover, it is quite interesting to note that the rate of increase in θ_{max} with respect to Q_t is higher for non-uniform

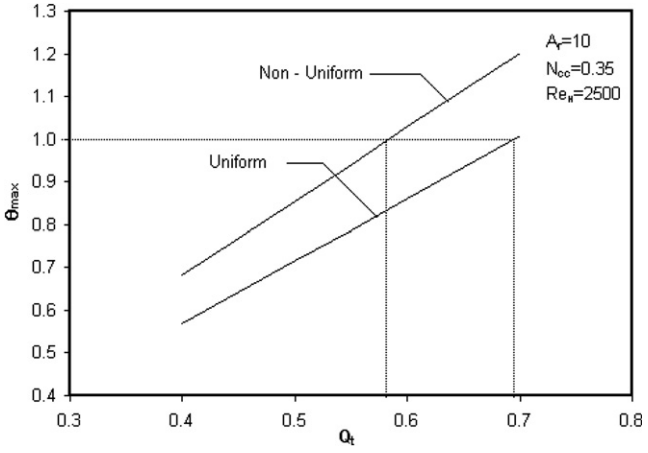

Fig. 10. Variation of the θ_{max} in the fuel element with Q_t for both uniform and non-uniform heat generation cases, at fixed values of $A_r = 10$, $N_{cc} = 0.35$, and $Re_H = 2500$.

volumetric energy generation than that of uniform volumetric energy generation case. Also, it is worth noting from this figure that other parameters being kept fixed, the critical value of Q_t for non-uniform volumetric energy generation in the fuel element is much less than that of uniform volumetric energy generation case. Thus, it can be concluded that although the non-uniform volumetric energy generation within the fuel element is somewhat realistic, it puts greater restriction on the fission energy to be generated as θ_{max} must not exceed its allowable limit.

Fig. 11 shows the variation of θ_{max} with Re_H for both uniform and non-uniform energy generation cases while A_r, N_{cc}, and Q_t are being kept fixed at 10.0, 0.35, and 0.50, respectively. As expected, it can be noticed from this figure that θ_{max} monotonically decreases with increase in Re_H, which is in good agreement with the physics of convective heat transfer. Also, it can be noted from this figure that for any fixed value of Re_H, other parameters being kept fixed, θ_{max} for non-uniform volumetric energy generation is considerably higher than that of uniform volumetric energy generation case and this is evidently more true for higher and higher fixed values of Re_H. Further, it can be easily noticed that the critical value of Re_H for non-uniform volumetric energy generation is much higher than that of uniform volumetric energy generation case. From the preceding discussion, it can be concluded that the non-uniform volumetric energy generation in the fuel element demands higher rate of coolant flow rate as compared to uniform volumetric energy generation case which, in turn, implies that the pumping power requirement of the coolant for non-uniform volumetric energy generation is much greater than that of uniform volumetric energy generation case.

4.3. Average Nusselt number

Fig. 12 depicts the variation of Nu_H with A_r for both uniform and non-uniform volumetric energy generation cases while keeping $N_{cc} = 0.35, Q_t = 0.50$, and $Re_H = 2500$ as fixed. It can be seen that while Nu_H decreases marginally with increase in A_r for uniform volumetric energy generation case, a reverse trend in the variation of Nu_H with A_r for non-uniform energy generation is evident from this figure. Further, it is important to note that although the total energy generation parameter Q_t remains the same for both uniform and non-uniform cases, non-uniform volumetric energy generation within the fuel element gives rise to considerably higher surface heat dissipation rate and this is particularly true for higher and higher values of A_r.

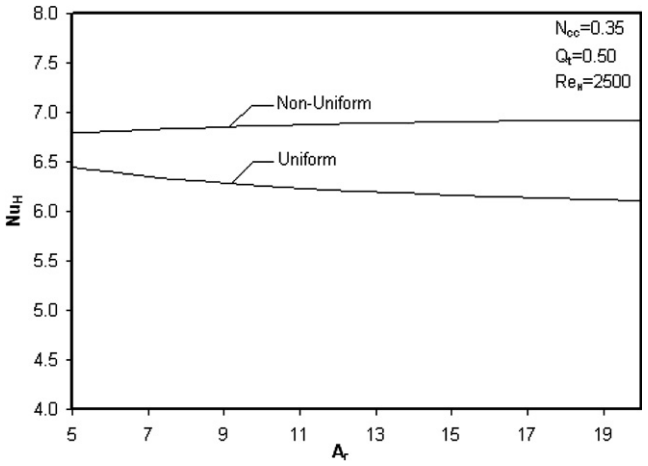

Fig. 12. Variation of Nu_H with A_r for both uniform and non-uniform heat generation cases, at fixed values of $N_{cc} = 0.35$, $Q_t = 0.50$, and $Re_H = 2500$.

Fig. 13 illustrates the variation of Nu_H with N_{cc} for both uniform and non-uniform volumetric energy generation cases while keeping $A_r = 10, Q_t = 0.50$, and $Re_H = 2500$ as fixed. It is surprising to note that irrespective of the manner in which the energy is generated in the fuel element, Nu_H is found to be almost independent of N_{cc}. However, for any fixed value of N_{cc}, non-uniform volumetric energy generation facilitates higher energy dissipation rate from

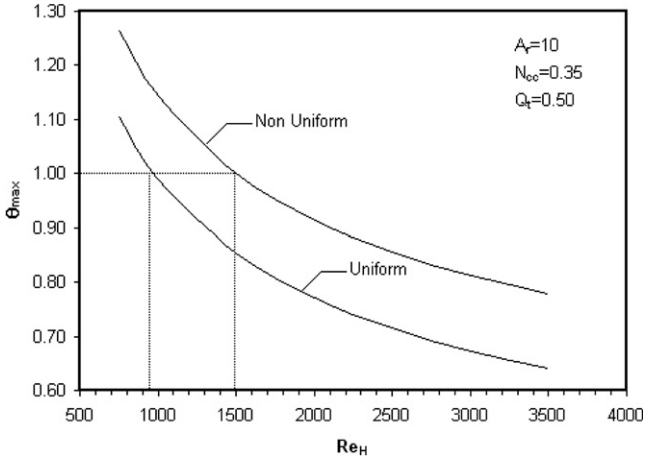

Fig. 11. Variation of the θ_{max} in the fuel element with Re_H for both uniform and non-uniform heat generation cases, at fixed values of $A_r = 10$, $N_{cc} = 0.35$, and $Q_t = 0.50$.

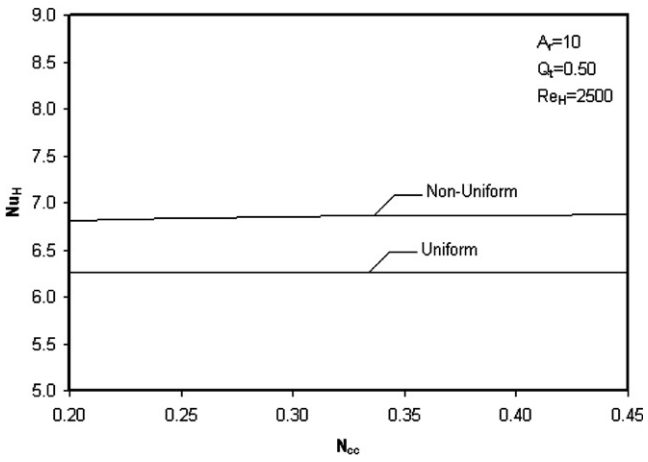

Fig. 13. Variation of Nu_H with N_{cc} for both uniform and non-uniform heat generation cases, at fixed values of $A_r = 10$, $Q_t = 0.50$, and $Re_H = 2500$.

the fuel element as compared to uniform volumetric energy generation case. Fig. 14 shows the variation of Nu_H with Q_t for both uniform and non-uniform volumetric energy generation cases while keeping $A_r = 10, N_{cc} = 0.35$, and $Re_H = 2500$ as fixed. It is interesting to note that the nature of variation of Nu_H with Q_t are very much similar to those illustrated in Fig. 13 for the variation of Nu_H with N_{cc}.

Fig. 15 depicts the variation of Nu_H with Re_H for both uniform and non-uniform volumetric energy generation cases while $A_r = 10$, $N_{cc} = 0.35$, and $Q_t = 0.50$ are being kept fixed. As expected, it is evident from this figure that irrespective of mode of energy generation in the fuel element, Nu_H increases monotonically with increase in Re_H. Further, it is important to note that energy dissipation rate for non-uniform volumetric energy generation in the fuel element, coolant flow rate being the same, is considerably higher than that of uniform volumetric energy generation case. Furthermore, it is important to note that the difference in energy dissipation rates for uniform and non-uniform volumetric energy generation cases becomes greater and greater for larger and larger coolant flow rate.

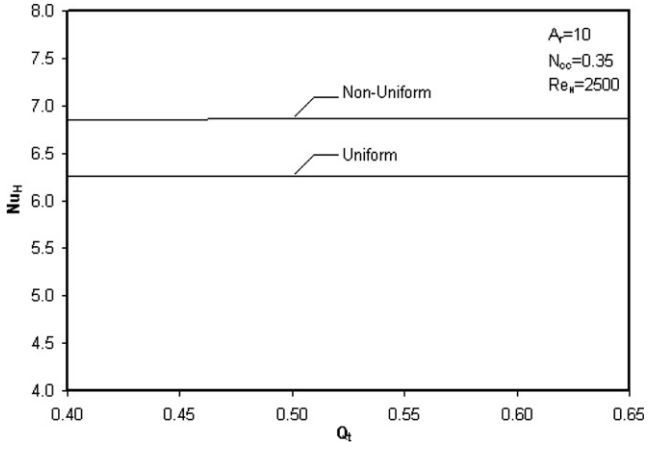

Fig. 14. Variation of Nu_H with Q_t for both uniform and non-uniform heat generation cases, at fixed values of $A_r = 10$, $N_{cc} = 0.35$, and $Re_H = 2500$.

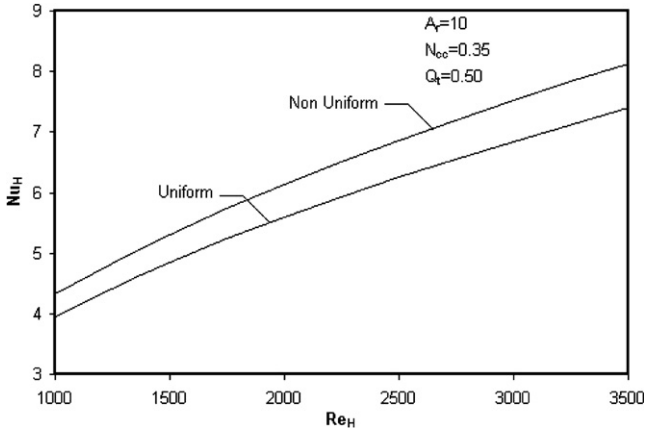

Fig. 15. Variation of Nu_H with Re_H for both uniform and non-uniform heat generation cases, at fixed values of $A_r = 10$, $N_{cc} = 0.35$, and $Q_t = 0.50$.

5. Conclusions

The objective of the present numerical study is of twofold – the first and the foremost objective is to carry out a comparative study of uniform and non-uniform volumetric energy generation in a rectangular nuclear fuel element and the second objective is to ascertain the values of critical design parameters, which govern the optimum but safe operating conditions of nuclear reactors having non-uniform volumetric energy generation. Accordingly, for both uniform as well as non-uniform volumetric energy generation cases, the boundary layer equations governing the flow and thermal fields in the fluid domain are solved numerically along with two-dimensional heat conduction equation in the solid domain by satisfying the conditions of continuity of temperature and heat flux at the solid–fluid interface. Keeping the value of Pr for liquid sodium to be constant at 0.005, numerical results are presented and discussed in detail for a wide range of parameters A_r, N_{cc}, Q_t and Re_H. It is concluded that for the same magnitude of total energy generated within the fuel element, a relatively more realistic non-uniform volumetric energy generation situation puts greater restriction on the power generation capacity of the nuclear reactor as compared to idealistic uniform volumetric energy generation case. It is also found that regardless of the total energy generation within the fuel element being the same for both uniform and non-uniform cases, the latter gives rise to considerably higher energy dissipation rate from the surface of the fuel element.

References

[1] T.L. Perelman, On conjugated problems of heat transfer, Int. J. Heat Mass Transfer 3 (1961) 293–303.
[2] R. Karvinen, Some new results for conjugated heat transfer in a flat plate, Int. J. Heat Mass Transfer 21 (1978) 1261–1264.
[3] K. Velusamy, V.K. Garg, Transient natural convection over a heat generating vertical cylinder, Int. J. Heat Mass Transfer 35 (5) (1992) 1293–1306.
[4] M. Wang, J.G. Georgiadis, Conjugate forced convection in crossflow over a cylinder array with volumetric heating, Int. J. Heat Mass Transfer 39 (1996) 1351–1361.
[5] G. Jilani, S. Jayaraj, M.A. Ahmed, Conjugate forced convection conduction heat transfer analysis of a heat generating vertical cylinder, Int. J. Heat Mass Transfer 45 (2002) 331–341.
[6] S. Jahangeer, M.K. Ramis, G. Jilani, Conjugate heat transfer analysis of a heat generating vertical plate, Int. J. Heat Mass Transfer 50 (2007) 85–93.
[7] M.M. El-Wakil, Nuclear Power Engineering, McGraw-Hill Book Company, Inc., New York, 1962.
[8] R.W. Hornbeck, Numerical Marching Techniques in Fluid Flows with Heat Transfer, NASA, Washington, DC, 1973.
[9] M. Vynnycky, S. Kimura, K. Kanev, I. Pop, Forced convection heat transfer from a flat plate: the conjugate problem, Int. J. Heat Mass Transfer 41 (1998) 45–59.